Letter

Energy-time entanglement coexisting with fiber-optical communication in the telecom *C* band

Yun-Ru Fan,[1] Yue Luo,[1] Zi-Chang Zhang,[1] Yun-Bo Li,[2] Sheng Liu,[2] Dong Wang,[2] De-Chao Zhang,[2] Guang-Wei Deng,[1] You Wang,[1,3] Hai-Zhi Song,[1,3] Zhen Wang,[4] Li-Xing You,[4] Chen-Zhi Yuan,[1,*] Guang-Can Guo,[1,5] and Qiang Zhou[1,5,†]

[1]*Institute of Fundamental and Frontier Sciences, University of Electronic Science and Technology of China, Chengdu 610054, China*

[2]*Department of Fundamental Network Technology, China Mobile Research Institute, Beijing 100053, China*

[3]*Southwest Institute of Technical Physics, Chengdu 610041, China*

[4]*Shanghai Institute of Microsystem and Information Technology, Chinese Academy of Sciences, Shanghai 200050, China*

[5]*CAS Key Laboratory of Quantum Information, University of Science and Technology of China, Hefei 230026, China*

(Received 25 May 2023; accepted 11 August 2023; published 24 August 2023)

We study the coexistence of energy-time entanglement with fiber-optical communication in the telecom *C* band. The property of noise from wavelength-multiplexed classical channels is characterized with different wavelength settings. With the largest noise, i.e., the worst case, we measure the entanglement property of the distributed energy-time entangled photon pairs at different data rates of fiber-optical communication. After being distributed over 40-km spooled fiber coexisting with a bidirectional data rate of 20 Gbps, a visibility of $82.01 \pm 1.10\%$ is obtained by measuring the Franson interference. With the Bennett-Brassard-Mermin 1992 (BBM92) protocol, a secret key rate of 343 bits per second is reached over the 40-km spooled fiber coexisting with a bidirectional data rate of 10 Gbps. Our result paves the way for developing a cost-effective quantum entanglement network compatible with fiber communication systems.

DOI: 10.1103/PhysRevA.108.L020601

Quantum communication, which is essential for building a quantum network, is drawing more and more attention [1–5]. Recently, it has been developed rapidly with fiber-optical communication infrastructures, in which quantum states are distributed via fiber-based quantum channels with the classical information exchanged via classical ones [6–8]. Up to now, most of these systems have been demonstrated with individual fiber links, i.e., quantum and classical channels in different fibers, to protect the fragile property of the quantum signal at the single-photon level. However, this is not a viable option under stringent operational expenditures or fiber-scarce conditions for scalable quantum networks. Towards this end, in 1997 Townsend put forward a scheme for the simultaneous transmission of quantum key distribution (QKD) signals and conventional data signals over the same piece of installed fiber using the wavelength-division multiplexing (WDM) technique [9]. A series of investigations on the coexistence of quantum and classical signals in the same piece of fiber have been implemented with the WDM and time-division multiplexing techniques [10–19]. Among these demonstrations, quantum entanglement coexisting with classical light is robust to noise owing to its quantum correlation property, which is important for developing quantum entanglement-based quantum networks [20–23]. For instance, by tightly filtering in time and frequency domains, polarization-entangled photon pairs can propagate, coexisting with classical light over 45-km installed fiber [24,25]. Compared with the polarization entanglement [25–27], energy-time entanglement is more robust to polarization decoherence in fiber-based quantum networks [28–30], while its coexistence in the same fiber with classical light has yet to be investigated.

In this Letter, we demonstrate a communication system for the coexistence of energy-time entanglement with fiber-optical communication using the WDM technique in the telecom *C* band. In our experiment, we observe the property of Raman noise from the classical channel and measure the quantum correlation of distributed quantum entangled photon pairs with different noise photons. After distributing over 40-km spooled fiber coexisting with bidirectional fiber-optical communication, a visibility of greater than $82.01 \pm 1.10\%$ is obtained in a Franson interferometer. Performances of entanglement-based QKD are analyzed with the Bennett-Brassard-Mermin 1992 (BBM92) protocol, showing a secret key rate (SKR) of 343 bits per second with a quantum bit error rate (QBER) of 8.61% at a bidirectional data rate of 10 Gbps. Our demonstration indicates the potential for developing a cost-effective quantum entanglement network coexisting with fiber-optical communication over the same piece of fiber.

A conceptual scheme of the coexistence of entanglement with fiber-optical communication is shown in Fig. 1(a). Alice and Bob send and receive a fiber-optical communication signal—as classical transceivers—through a classical channel. Meanwhile, they also receive quantum signals—as quantum receivers—from the quantum center through a quantum channel. Alice and Bob are connected by using the same piece of fiber link, in which the fiber-optical communication and quantum entanglement distribution coexist by using the WDM technique, i.e., the classical channel and quantum channel are located at different wavelengths. Two WDM devices—as a classical-quantum combiner—are used to multiplex the

*c.z.yuan@uestc.edu.cn
†zhouqiang@uestc.edu.cn

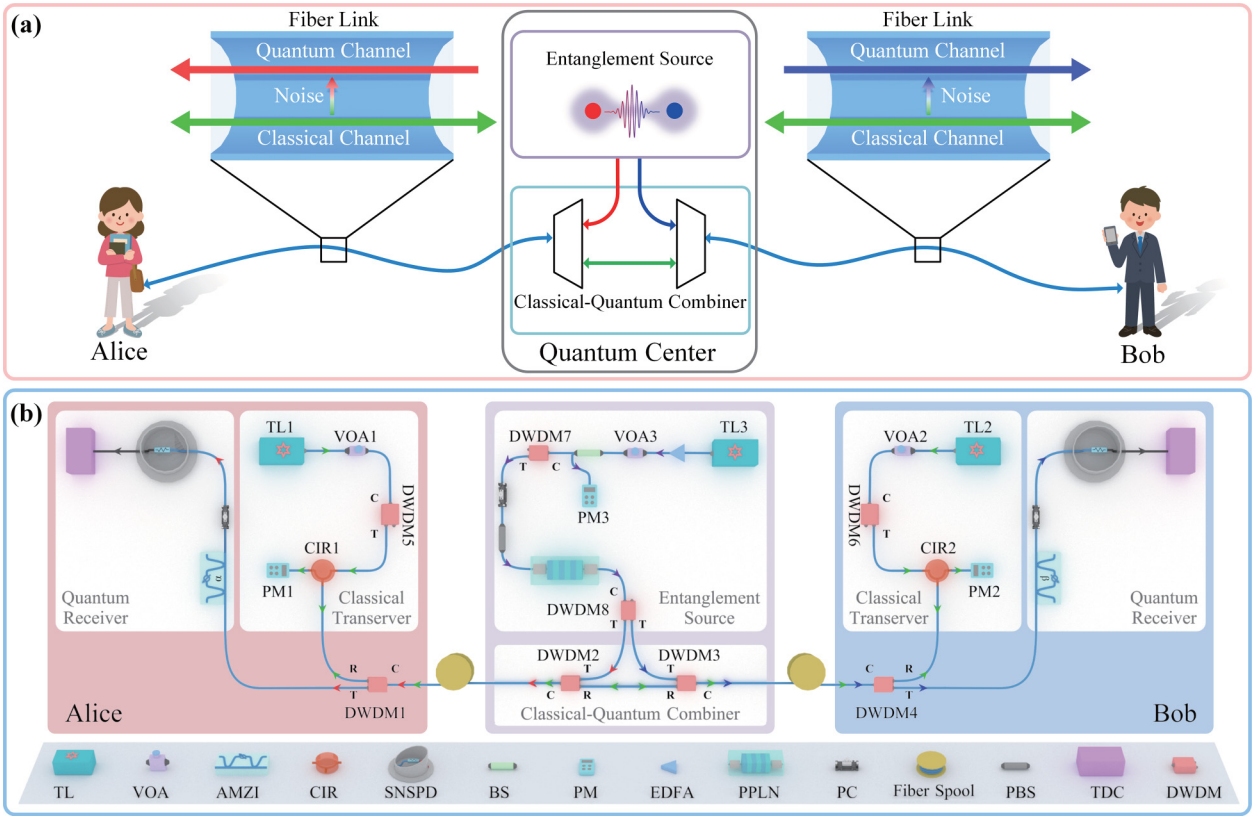

FIG. 1. Scheme of energy-time entanglement coexisting with fiber-optical communication in the telecom *C* band. (a) Conceptual scheme of the coexistence of entanglement with fiber-optical communication. A quantum center, consisting of a quantum entanglement source and DWDMs for generating and distributing quantum entangled photon pairs to Alice and Bob. (b) Experimental setup for the coexistence of entanglement distribution with fiber-optical communication along 40-km spooled fiber. TL: tunable laser; VOA: variable optical attenuator; AMZI: asymmetrical Mach-Zehnder interferometer; CIR: circulator; BS: beam splitter; EDFA: erbium-doped fiber amplifier; PPLN: periodically poled lithium niobate; PC: polarization controller; PBS: polarization beam splitter; SNSPD: superconductor nanowire single-photon detector; TDC: time-to-digital converter; DWDM: dense wavelength-division multiplexing. Note that DWDM1–DWDM7 have three ports (C: common; T: transmit; R: reflect); DWDM1 (DWDM2/3/4) transmits photons in ITU channel C35 (C57) with a bandwidth of 100 GHz; DWDM8 has four ports—two T ports for ITU channels C35 and C57, respectively.

fiber-optical communication data and quantum entangled photon pairs in a quantum center. Although the setup effectively prevents the quantum channel from being contaminated by the classical channel, the Raman noise photons generated by the fiber-optical communication data within the spectral region of the quantum channel inevitably influence the property of distributed quantum entanglement. Fortunately, the quantum correlation could help entangled photon pairs to tolerate more background noise than single-photon-based quantum information applications. In our experiment, we experimentally show that by employing the WDM technique and coincidence detection we extract quantum entanglement from the coexisting noise photons and apply it for entanglement-based QKD with the BBM92 protocol.

Our experimental setup is shown in Fig. 1(b). In the experiment, the fiber-optical communication signal from a tunable laser at Alice (Bob), i.e., TL1 (TL2) at a wavelength of λ_c, is sent to a fiber link after propagating through a variable optical attenuator VOA1 (VOA2), a dense wavelength-division multiplexing DWDM5 (DWDM6) device, and a circulator CIR1 (CIR2). The VOA1 and VOA2 are used to adjust the data rates of the coexisting fiber-optical communication that is monitored by PM1 and PM2 at port 3 of CIR1 and CIR2, respectively. DWDM5 and DWDM6 are employed to suppress the background noise from TL1 and TL2, while CIR1 and CIR2 isolate the bidirectional classical signals. Entangled photon pairs are generated through the cascaded second-harmonic generation (SHG) and spontaneously parametric down-conversion (SPDC) processes in a single piece of a periodically poled lithium niobate (PPLN) waveguide [31], which is pumped by TL3 at a wavelength of $\lambda_l = 1540.56$ nm [International Telecommunication Union (ITU) channel of C46]. The pump light power is amplified, attenuated, and monitored using an erbium-doped fiber amplifier (EDFA), VOA3, and a 99:1 beam splitter (BS), respectively. DWDM7 is employed to suppress noise photons from the pump laser and the EDFA. A polarization controller (PC) and a polarization beam splitter (PBS) are used to manipulate and monitor the polarization state of the pump light and ensure polarization alignment for phase matching in the PPLN waveguide. DWDM8 is used to select signal and idler photon pairs, which are at $\lambda_s = 1549.32$ nm and $\lambda_i = 1531.90$ nm, i.e., the C57 and C35 channels, respectively. Then the signal (idler) photons and coexisting fiber-optical communication signal are multiplexed and sent

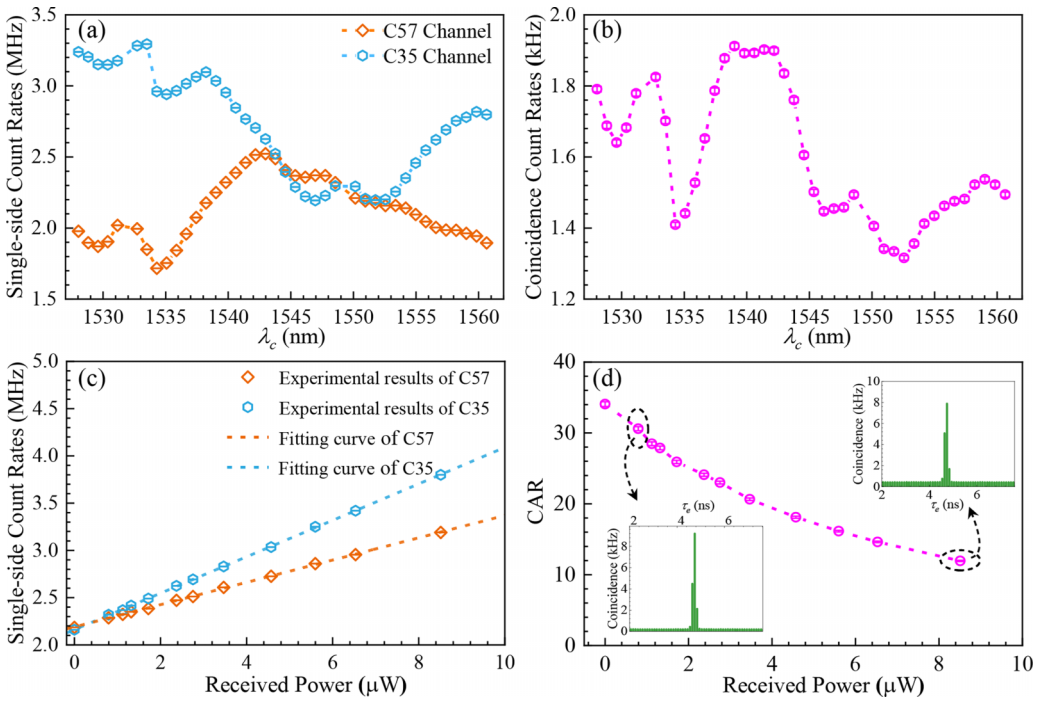

FIG. 2. Experimental results of Raman noises in a quantum channel. (a) Single-side count rates of noise photons at C35 and C57 channels with a unidirectional fiber-optical communication signal at different wavelengths. (b) Coincidence count rates of noise photons between C35 and C57 channels with a unidirectional fiber-optical communication signal at different wavelengths. (c) Single-side count rates of a photon in a quantum channel with different powers of a fiber-optical communication signal at 1538.98 nm. (d) CAR of photon pairs in a quantum channel with different powers of a fiber-optical communication signal at 1538.98 nm.

into the same fiber links via DWDM2 (DWDM3), respectively. After transmitting through a 20-km-long fiber link and DWDM1 (DWDM4), the signal (idler) photons enter an asymmetrical Mach-Zehnder interferometer (AMZI) to measure their property of energy-time entanglement. The photons outputted from the AMZI are detected and recorded by superconductor nanowire single-photon detectors (SNSPDs) and a time-to-digital converter (TDC). The coexisting fiber-optical communication signal from Alice (Bob) to Bob (Alice) outputs from the transmission (T) port of DWDM4 (DWDM1). The data rate of the received fiber-optical communication signal is measured at $R \times 2$ ($R \times 1$) by using PM2 (PM1) at Bob (Alice) as shown in Fig. 1(b).

To investigate the property of noise from the fiber-optical communication channel, we measure the single-side count rate of the Raman noise photons at C35 and C57 with unidirectional fiber-optical communication signals at different wavelengths. In this case, the quantum entanglement source is disconnected at the quantum center. When the classical signal is unidirectional from Alice to Bob, the measured results are shown in Fig. 2(a), i.e., blue and orange dots, respectively. The laser power is adjusted so that the receiver obtains a power of −24 dBm, i.e., minimum required power for a data rate of 20 Gbps. The coincidence count rates of noise photons from C35 and C57 channels are also measured with a unidirectional data rate of 20 Gbps at different wavelengths. The experimental results are shown in Fig. 2(b). It can be seen that a maximum coincidence count rate is obtained with a classical signal at a wavelength of 1538.98 nm, which corresponds to the largest noise in our experiment. Under this condition, we further investigate the properties of the distributed energy-time entangled photon pairs at different data rates at 1538.98 nm, i.e., different monitored optical power in PM1 and PM2. The measured single-side count rates in quantum channels are shown in Fig. 2(c). Without any coexisting classical signal, the single-side count rates of both the signal and idler photons are 2.2 MHz. With an increase of data rates, the single-side

TABLE I. Performances of quantum key distribution with different data rates.

Data rate	Visibility $\beta_1 = -\pi/2$	Visibility $\beta_2 = -6\pi/5$	Raw key rate	QBER	Secret key rate
0 Gbps	88.51 ± 1.71%	89.31 ± 1.24%	4668 bps	6.60%	1065 bps
5 Gbps	87.28 ± 1.21%	87.60 ± 2.12%	4712 bps	7.26%	818 bps
10 Gbps	85.33 ± 0.83%	84.85 ± 2.07%	4831 bps	8.61%	343 bps
20 Gbps	82.01 ± 1.10%	82.49 ± 2.20%	5004 bps	9.86%	

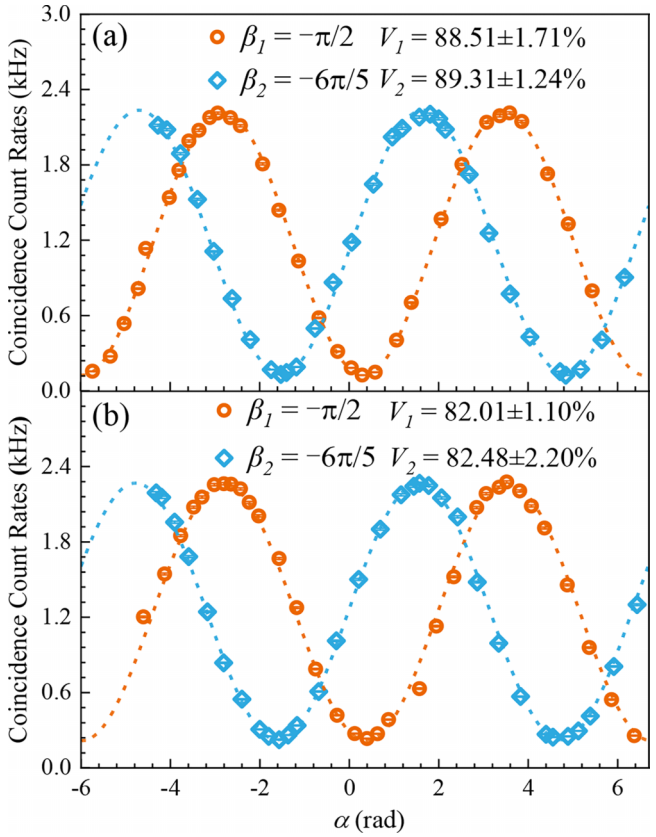

FIG. 3. Quantum entanglement distribution coexisting with fiber-optical communication. (a) Franson interference curves of energy-time entanglement without any coexisting classical signal. (b) Franson interference curves coexisting with 20 Gbps bidirectional fiber-optical communication.

count rates exhibit a linear increase, which is consistent with the increase of the Raman noise photons. Figure 2(d) shows the decrease of the coincidence to accidental coincidence rate (CAR) with an increase of data rates. The inset of Fig. 2(d) gives the histogram of coincidence counts with bidirectional received powers of −20 and −31 dBm, respectively.

We measure the entanglement property of energy-time entangled photon pairs after being distributed from the quantum center to Alice and Bob in our experiment. At Alice the phase α is scanned with a fixed phase β at Bob. Without any coexisting classical signal, the Franson interference curves for $\beta = -\pi/2$ and $\beta = -6\pi/5$ are shown in Fig. 3(a) with visibilities of $V_1 = 89.31 \pm 1.24\%$ and $V_2 = 88.51 \pm 1.71\%$, respectively. Note that the imperfect visibilities come from the multiphoton events of the photon pairs and the imperfection of the two AMZIs [32,33]. With a bidirectional data rate of 20 Gbps, the results of the Franson interference are shown in Fig. 3(b) with visibilities of $V_1 = 82.01 \pm 1.10\%$ and $V_2 = 82.49 \pm 2.20\%$, respectively. The visibilities of the Franson interference curves at different data rates are measured and summarized in Table I. The results show that visibilities decrease with the data rates due to the generated Raman noise in the fiber. Furthermore, we analyze the property of energy-time entanglement-based QKD coexisting with fiber-optical communication using the BBM92 protocol. In our experiment, with a bidirectional data rate of 10 Gbps, a raw key rate (n_{sift}) of 4831 bps is obtained from the coincidence measurements. With the lowest visibility of 82.78%, we obtain a QBER of 8.61% which is calculated by QBER = (1 − Visibility)/2. The SKR is 343 bps from SKR $\geqslant n_{\text{sift}}[1 - 2.2H_2(x)]$, where $H_2(x)$ is the binary entropy function, $H_2(x) = -x\log_2 x - (1-x)\log_2(1-x)$; x is the QBER [34,35]. The performances of our entanglement-based QKD at different data rates are summarized in Table I.

In conclusion, we have demonstrated energy-time entanglement coexisting with fiber-optical communication in the telecom *C* band. Enabled by the quantum correlation of entangled photon pairs and the wavelength-division multiplexing technique, the distribution of energy-time entanglement coexisting with fiber-optical communication at a bidirectional data rate of 20 Gbps is achieved over 40-km spooled fiber, in which a visibility of $82.01 \pm 1.10\%$ is measured in the Franson interferometer. With the BBM92 protocol, we have reached an SKR of 343 bps with a QBER of 8.61% coexisting with fiber-optical communication at a bidirectional data rate of 10 Gbps. Our results pave the way for the development of a cost-effective quantum entanglement network coexisting with fiber-optical communication in the same fiber. In the future, the performance of our communication system could be improved by developing a bright integrated quantum light source, reducing the imperfection of the Franson interferometer, and extending the degrees of freedom of the photons for multiplexing.

This work is supported by Sichuan Science and Technology Program (Grants No. 2021YFSY0063, No. 2021YFSY0062, No. 2021YFSY0064, No. 2021YFSY0065, No. 2021YFSY0066, No. 2022YFSY0061, No. 2022YFSY0062, and No. 2022YFSY0063); National Key Research and Development Program of China (Grants No. 2018YFA0307400 and No. 2018YFA0306102); National Natural Science Foundation of China (Grants No. U19A2076 and No. 62005039); and Innovation Program for Quantum Science and Technology (Grant No. 2021ZD0301702).

[1] N. Gisin, G. Ribordy, W. Tittel, and H. Zbinden, Quantum cryptography, Rev. Mod. Phys. **74**, 145 (2002).

[2] H. J. Kimble, The quantum internet, Nature (London) **453**, 1023 (2008).

[3] S. Wengerowsky, S. K. Joshi, F. Steinlechner, H. Hübel, and R. Ursin, An entanglement-based wavelength-multiplexed quantum communication network, Nature (London) **564**, 225 (2018).

[4] S. Wehner, D. Elkouss, and R. Hanson, Quantum internet: A vision for the road ahead, Science **362**, eaam9288 (2018).

[5] S.-H. Wei, B. Jing, X.-Y. Zhang, J.-Y. Liao, C.-Z. Yuan, B.-Y. Fan, C. Lyu, D.-L. Zhou, Y. Wang, G.-W. Deng *et al.*, Towards real-world quantum networks: A review, Laser Photonics Rev. **16**, 2100219 (2022).

[6] H.-L. Yin, T.-Y. Chen, Z.-W. Yu, H. Liu, L.-X. You, Y.-H. Zhou, S.-J. Chen, Y. Mao, M.-Q. Huang, W.-J. Zhang *et al.*,

Measurement-Device-Independent Quantum Key Distribution Over a 404 km Optical Fiber, Phys. Rev. Lett. **117**, 190501 (2016).

[7] J. Qiu, Quantum communications leap out of the lab, Nature (London) **508**, 441 (2014).

[8] Y.-L. Tang, H.-L. Yin, Q. Zhao, H. Liu, X.-X. Sun, M.-Q. Huang, W.-J. Zhang, S.-J. Chen, L. Zhang, L.-X. You *et al.*, Measurement-Device-Independent Quantum Key Distribution over Untrustful Metropolitan Network, Phys. Rev. X **6**, 011024 (2016).

[9] P. D. Townsend, Simultaneous quantum cryptographic key distribution and conventional data transmission over installed fibre using wavelength-division multiplexing, Electron. Lett. **33**, 188 (1997).

[10] I. Choi, R. J. Young, and P. D. Townsend, Quantum key distribution on a 10 Gb/s WDM-PON, Opt. Express **18**, 9600 (2010).

[11] P. Eraerds, N. Walenta, M. Legré, N. Gisin, and H. Zbinden, Quantum key distribution and 1 Gbps data encryption over a single fibre, New J. Phys. **12**, 063027 (2010).

[12] R.-J. Essiambre, G. Kramer, P. J. Winzer, G. J. Foschini, and B. Goebel, Capacity limits of optical fiber networks, J. Lightwave Technol. **28**, 662 (2010).

[13] K. A. Patel, J. F. Dynes, I. Choi, A. W. Sharpe, A. R. Dixon, Z. L. Yuan, R. V. Penty, and A. J. Shields, Coexistence of High-Bit-Rate Quantum Key Distribution and Data on Optical Fiber, Phys. Rev. X **2**, 041010 (2012).

[14] K. Patel, J. Dynes, M. Lucamarini, I. Choi, A. Sharpe, Z. Yuan, R. Penty, and A. Shields, Quantum key distribution for 10 Gb/s dense wavelength division multiplexing networks, Appl. Phys. Lett. **104**, 051123 (2014).

[15] L.-J. Wang, L.-K. Chen, L. Ju, M.-L. Xu, Y. Zhao, K. Chen, Z.-B. Chen, T.-Y. Chen, and J.-W. Pan, Experimental multiplexing of quantum key distribution with classical optical communication, Appl. Phys. Lett. **106**, 081108 (2015).

[16] R. Kumar, H. Qin, and R. Alléaume, Coexistence of continuous variable QKD with intense DWDM classical channels, New J. Phys. **17**, 043027 (2015).

[17] R. Valivarthi, P. Umesh, C. John, K. A. Owen, V. B. Verma, S. W. Nam, D. Oblak, Q. Zhou, and W. Tittel, Measurement-device-independent quantum key distribution coexisting with classical communication, Quantum Sci. Technol. **4**, 045002 (2019).

[18] R. C. Berrevoets, T. Middelburg, R. F. Vermeulen, L. D. Chiesa, F. Broggi, S. Piciaccia, R. Pluis, P. Umesh, J. F. Marques, W. Tittel *et al.*, Deployed measurement-device independent quantum key distribution and Bell-state measurements coexisting with standard internet data and networking equipment, Commun. Phys. **5**, 186 (2022).

[19] J. Wang, B. J. Rollick, Z. Jia, H. Zhang, and B. A. Huberman, Time-interleaving enabled co-propagation of QKD and classical channels over 100-km fiber with 10-dBm classical launch power, arXiv:2304.13828.

[20] S. K. Joshi, D. Aktas, S. Wengerowsky, M. Lončarić, S. P. Neumann, B. Liu, T. Scheidl, G. C. Lorenzo, Ž. Samec, L. Kling *et al.*, A trusted node–free eight-user metropolitan quantum communication network, Sci. Adv. **6**, eaba0959 (2020).

[21] W. Wen, Z. Chen, L. Lu, W. Yan, W. Xue, P. Zhang, Y. Lu, S. Zhu, and X.-s. Ma, Realizing an Entanglement-Based Multiuser Quantum Network with Integrated Photonics, Phys. Rev. Appl. **18**, 024059 (2022).

[22] S. Shen, C. Yuan, Z. Zhang, H. Yu, R. Zhang, C. Yang, H. Li, Z. Wang, Y. Wang, G. Deng *et al.*, Hertz-rate metropolitan quantum teleportation, Light: Sci. Appl. **12**, 115 (2023).

[23] S.-H. Wei, B. Jing, X.-Y. Zhang, J.-Y. Liao, H. Li, L.-X. You, Z. Wang, Y. Wang, G.-W. Deng, H.-Z. Song *et al.*, Storage of 1650 modes of single photons at telecom wavelength, arXiv:2209.00802.

[24] W. Wu, J. Chung, G. Kanter, N. Lauk, R. Valivarthi, R. R. Ceballos, C. Pena, N. Sinclair, J. M. Thomas, E. M. Eastman *et al.*, Illinois express quantum network for distributing and controlling entanglement on metro-scale, in *2021 IEEE/ACM Second International Workshop on Quantum Computing Software (QCS)* (IEEE, New York, 2021), pp. 35–42.

[25] J. M. Thomas, G. S. Kanter, E. M. Eastman, K. F. Lee, and P. Kumar, Entanglement distribution in installed fiber with coexisting classical light for quantum network applications, in *Optical Fiber Communication Conference (OFC) 2022*, edited by S. Matsuo, D. Plant, J. Shan Wey, C. Fludger, R. Ryf, and D. Simeonidou, Technical Digest Series (Optica Publishing Group, Washington, DC, 2022), paper Tu3I.3.

[26] J. Chung, E. M. Eastman, G. S. Kanter, K. Kapoor, N. Lauk, C. H. Pena, R. K. Plunkett, N. Sinclair, J. M. Thomas, R. Valivarthi *et al.*, Design and implementation of the Illinois express quantum metropolitan area network, IEEE Trans. Quantum Eng. **3**, 4100920 (2022).

[27] J. M. Thomas, G. S. Kanter, and P. Kumar, Designing noise-robust quantum networks coexisting in the classical fiber infrastructure, arXiv:2304.09076.

[28] A. Cuevas, G. Carvacho, G. Saavedra, J. Cariñe, W. Nogueira, M. Figueroa, A. Cabello, P. Mataloni, G. Lima, and G. Xavier, Long-distance distribution of genuine energy-time entanglement, Nat. Commun. **4**, 2871 (2013).

[29] P. Lefebvre, R. Valivarthi, Q. Zhou, L. Oesterling, D. Oblak, and W. Tittel, Compact energy–time entanglement source using cascaded nonlinear interactions, J. Opt. Soc. Am. B **38**, 1380 (2021).

[30] C. Yuan, H. Yu, Z. Zhang, Y. Wang, H. Li, L. You, Y. Wang, H. Song, G. Deng, and Q. Zhou, Quantum entanglement distribution coexisting with classical fiber communication, in *Asia Communications and Photonics Conference (ACPC) 2019*, OSA Technical Digest (Optica Publishing Group, Washington, DC, 2019), paper T2F.2.

[31] Z. Zhang, C. Yuan, S. Shen, H. Yu, R. Zhang, H. Wang, H. Li, Y. Wang, G. Deng, Z. Wang *et al.*, High-performance quantum entanglement generation via cascaded second-order nonlinear processes, npj Quantum Inf. **7**, 123 (2021).

[32] J. D. Franson, Bell Inequality for Position and Time, Phys. Rev. Lett. **62**, 2205 (1989).

[33] W. Tittel, J. Brendel, N. Gisin, and H. Zbinden, Long-distance Bell-type tests using energy-time entangled photons, Phys. Rev. A **59**, 4150 (1999).

[34] X. Ma, C.-H. F. Fung, and H.-K. Lo, Quantum key distribution with entangled photon sources, Phys. Rev. A **76**, 012307 (2007).

[35] J. Yin, Y. Cao, Y.-H. Li, J.-G. Ren, S.-K. Liao, L. Zhang, W.-Q. Cai, W.-Y. Liu, B. Li, H. Dai *et al.*, Satellite-to-Ground Entanglement-Based Quantum Key Distribution, Phys. Rev. Lett. **119**, 200501 (2017).